CHINESE JOURNAL OF CATALYSIS
Volume 32, Issue 3, 2011
Online English edition of the Chinese language journal

Available online at www.sciencedirect.com
ScienceDirect

Cite this article as: Chin J Catal, 2011, 32: 418–427.

RESEARCH PAPER

Hydrothermal Stability of Meso-microporous Composites and Their Catalytic Cracking Performance

HAN Wei, JIA Yuxin, XIONG Guoxing*, YANG Weishen#

State Key Laboratory of Catalysis, Dalian Institute of Chemical Physics, Chinese Academy of Sciences, Dalian 116023, Liaoning, China

Abstract: Meso-microporous composites show great promise for catalysis because of their variously-sized porous structures. A series of composites containing uniform mesopores and MFI zeolitic channels were prepared by a template-free sol-gel method. The composite containing silicalite-1 structures was found to be much more hydrothermally stable than MCM-41. The composites with ZSM-5 structures showed higher catalytic activity and resistance to deactivation than commercial HZSM-5 in the catalytic cracking reaction of 1,3,5-triisopropylbenzene. The conversion and catalytic cracking product distribution of 1,3,5-triisopropylbenzene depended highly on the mesopore size of the composites. Higher conversions and small molecule cracking products were obtained using composites with smaller mesopores.

Key words: meso-microporous composite; MFI zeolite; hydrothermal stability; 1,3,5-triisopropylbenzene; catalytic cracking

Zeolites have been applied widely in many industrial processes such as adsorption and catalysis because of their high surface area, adsorption capacity, ion-exchange capacity, and regular arrays of channels and cavities (0.3–1.5 nm). Their intricate channel structures allow the zeolites to have different types of shape selectivity, i.e., for products, reactants, and transition states, which can be used to direct a given catalytic reaction toward the desired product and avoid undesired side reactions [1]. However, the small pore sizes of zeolites result in diffusion and mass transfer limitations especially in the reactions involving large molecules. Since the discovery of MCM-41 in 1992 [2,3], mesoporous materials have attracted much attention because of their potential use as catalysts and catalyst supports for the conversion of large molecules. Compared to conventional zeolites, mesoporous materials have low hydrothermal stability and acidity, which has been attributed to their amorphous pore walls [4].

Since meso-microporous composites can possibly combine the advantages of variously-sized porous structures, researchers have made many attempts to prepare meso-microporous composites. Pinnavaia et al. [5,6] and Xiao et al. [7,8] used surfactant to assemble zeolite precursor for synthesizing mesoporous materials with zeolitic walls. Zeolites with mesopores were also fabricated by the addition of different templates such as rigid templates containing carbon nanoparticles [9], carbon nanotubes [10] and carbon aerogels [11,12] or soft templates containing polymers [13,14] and surfactants [15,16] into the zeolite synthesis solution. As to template-free routes to the meso-microporous composite, steaming, acid-leaching dealumination [17], and alkali-leaching desilication [18] of zeolite crystals often generate mesopores with wide size distributions. In our previous work, we developed a template-free sol-gel method to synthesize a series of meso-microporous composites from a zeolite precursor sol. They were found to consist of interconnected worm-like mesopores or intercrystalline mesopores with irregular arrays and their mesopore sizes could be controlled between 2 and 30 nm [19–21]. In this work, we investigated the hydrothermal stability of several meso-microporous composites and their catalytic performance in the cracking reaction of 1,3,5-triisopropylbenzene.

Received 30 April 2010. Accepted 26 November 2010.
***Corresponding author.** Tel: +86-411-84379182; Fax: +86-411-84694447; E-mail: gxxiong@dicp.ac.cn
#Corresponding author. Tel: +86-411-84379073; Fax: +86-411-84694447; E-mail: yangws@dicp.ac.cn
Foundation item: Supported by SINOPEC (X503008) and the National Natural Science Foundation of China (20321303).

DOI: 10.1016/S1872-2067(10)60177-5

1 Experimental

1.1 Preparation of the meso-microporous composites

1.1.1 Preparation of the MFI zeolite precursor sol

In a typical silicalite-1 precursor sol synthesis, 20.4 g of the 20% aqueous solution of tetrapropylammonium hydroxide (TPAOH, Fluka) was added to 16.7 g of tetraethyl orthosilicate (TEOS, 98%, Beijing Yili) under vigorous stirring. To the resulting emulsion, 19.8 g of twice distilled water was added. The resulting emulsion with the molar composition of 1.0TEOS:0.25TPAOH:25H_2O was stirred at 50 °C for 48 h to form a clear silicalite-1 precursor sol.

25.4 g of the 20% aqueous solution of TPAOH was added to the mixture of 20.8 g of TEOS and 0.4 g of aluminum isopropoxide (Al(*i*-OPr)$_3$, 99.5%, Tianjin Jinke) under vigorous stirring at room temperature to obtain a turbid solution with the molar composition of 1.0TEOS: 0.02Al(*i*-OPr)$_3$:0.25TPAOH: 11.3H_2O. Clear ZSM-5 precursor sol was obtained by stirring the turbid solution at 50 °C for 48 h.

1.1.2 Preparation of the MFI zeolite precursor xerogel

Silicalite-1 and the ZSM-5 precursor sol were transferred to clean glass dishes and dried at 30 °C in a vacuum box at 6.67 kPa until they became xerogels. The silica contents in the silicalite-1 and ZSM-5 xerogels were 7.0×10^{-3} mol/g and 7.7×10^{-3} mol/g, respectively.

1.1.3 Solvo/hydrothermal crystallization of the xerogel

Glycerol (≥ 99.0%, Anshan Zhiao), glycol (99.8%, Tianjin Bodi), and twice distilled water were used as media for heat crystallization. A mixture of xerogel and solvent/water (1 SiO_2: 150 solvent/water molar ratio) was transferred into Teflon-lined stainless steel autoclaves and solvo/hydrothermal crystallization was carried out at a certain temperature for 24 h. The solid products were filtered, washed, dried at 30 °C in a vacuum box, and calcined in air at 550 °C for 6 h. The calcined samples were designated S-X-*y* or Z-X-*y* (S and Z indicate silicalite-1 and ZSM-5 xerogels, respectively; X represents the crystallization medium such as G = glycerol, A = glycol, and W = water; *y* is the crystallization temperature). For example, S-G-130 was the sample prepared by crystallizing silicalite-1 xerogel and glycerol at 130 °C. We prepared five meso-microporous composites: S-G-130, Z-G-130, Z-A-130, Z-A-180, and Z-W-100.

1.2 Preparation of mesoporous MCM-41

Mesoporous MCM-41 was also synthesized for comparison. 0.3 g of sodium hydroxide (NaOH, ≥ 96.0%, Tianjin Kemiou) and 1.7 g of cetyltrimethylammonium bromide (CTAB, ≥ 99.0%, Shanghai Guoyao) were dissolved in 144 ml of twice distilled water at 40 °C followed by the addition of 8.3 g of TEOS at room temperature. The mixture was stirred for 15 min and transferred into a Teflon-lined stainless steel autoclave to carry out hydrothermal synthesis at 120 °C for 3 d. As-synthesized MCM-41 was filtered, washed, dried, and calcined in air at 550 °C for 6 h.

1.3 Characterization of the samples

The particle size distribution of the precursor sol was measured using a N4 plus laser scattering particle meter (Coulter) equipped with a 10 mW He-Ne laser. X-ray diffraction (XRD) characterization was performed using a Rigaku D/max-2500PC X-ray diffractometer with a copper target at 40 kV and 30 mA (2θ = 1°–10°) or 100 mA (2θ = 5°–50°) with the step size of 0.02°. Fourier transform infrared (FT-IR) spectra were recorded using a Nicolet Impact 410 FTIR spectrometer. A mixture of the sample and KBr was pressed into a thin wafer before the IR measurement. All IR spectra were measured under the following conditions: resolution of 4 cm^{-1}, scan time of 32, and scan range from 400 to 4000 cm^{-1}. N_2 adsorption/desorption isotherms of the samples were measured on a Coulter Omnisorp-100CX apparatus at –196 °C. The solid samples were first degassed at 350 °C under high vacuum (1.33×10^{-4} Pa) for 3 h to remove adsorbed impurities from the pores of the samples before the isotherms were recorded. Mesopore and micropore size distributions were determined using BJH method from desorption branch and HK method from adsorption branch, respectively.

1.4 Hydrothermal stability and catalytic cracking performance

0.1 g of the calcined sample and 20 g of twice distilled water in a Teflon-lined stainless steel autoclave were heated at 180 °C for 12 h to test hydrothermal stability. The catalytic cracking reaction of 1,3,5-triisopropylbenzene over different samples was tested in a home-made pulse microreactor based on a HP 4890D GC system. 50 mg of the catalyst (40–60 mesh) was pretreated under a high purity nitrogen flow at 400 °C for 1 h. 0.1 μl of 1,3,5-triisopropylbenzene was pulse-injected and carried by high pure nitrogen at a flow rate of 20 ml/min into the catalyst layer at 400 °C. The cracking products were separated using a HP-5 capillary column (length: 15 m, inner diameter: 0.530 mm, thickness of liquid film: 1.50 μm) with a programmed-temperature process from 40 to 200 °C and detected by an FID detector at 250 °C.

2 Results and discussion

2.1 Particle size distribution of MFI zeolite precursor sol

Results from the laser scattering particle meter show that both the MFI zeolite precursor sols have a very uniform particle size distribution. For the silicalite-1 precursor sol, ca. 97% of the sol particles range between 6–12 nm and their mean size is 8.8 nm. For the ZSM-5 precursor sol, most of the sol particles (ca. 85%) have the size of 11.9 nm beside a small amount of larger sol particles with the size of 100 nm generated from the rapid hydrolysis and condensation processes of TEOS and Al(*i*-OPr)$_3$ in alkaline solution. de Moor et al. [22,23] observed two types of precursor particles (2.8 nm sized primary units and ~10 nm aggregates) in MFI zeolite synthesis systems by small-angle X-ray scattering. Based on these results, sol particles can be thought reasonably to be aggregates of zeolite primary units.

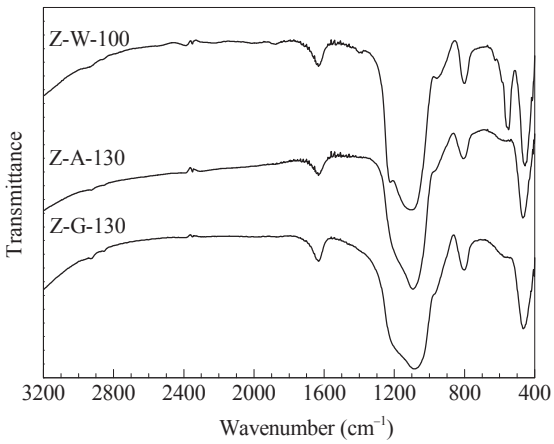

Fig. 2. FT-IR spectra of the studied samples.

2.2 XRD patterns and FT-IR spectra of the studied samples

XRD patterns of as-synthesized and calcined MCM-41 samples show several typical diffraction peaks between 1° and 6° (Fig. 1). They are similar to the XRD patterns reported in literature [3], which indicates that there are ordered mesoporous structures within these samples. It is different from the ordered mesoporous MCM-41 that no diffraction peaks below 5° appear in the XRD patterns of the meso-microporous composites. These meso-microporous composites do not have mesopores with an ordered array. Their XRD patterns, which are similar to Z-G-130 sample in Fig. 1, only contains wide diffraction peaks located between 15° and 30° except for Z-W-100 sample. The crystalline ordering of the zeolite structures within them is less than 4–5 unit cells or 8–10 nm [24]. Although their ordering is not adequate to be detected by XRD, the appearance of the 550–560 cm^{-1} band that corresponds to the double ring vibration in their FT-IR spectra (Fig. 2) verifies the existence of the MFI zeolite structures [25]. The XRD pattern for Z-W-100 sample that was prepared in water at 100 °C contains a series of typical ZSM-5 zeolite diffraction peaks. Z-W-100 sample has a crystal size of 50.4 nm in the vertical direction of (011) determined using the Scherrer equation.

2.3 Texture properties of the studied samples

The N_2 adsorption/desorption isotherms of meso-microporous composites can be assigned to type I and IV composites except for the Z-W-100 sample (Fig. 3). With a decrease in the number of OH within the crystallization medium molecules (from glycerol, glycol, to water), the hysteresis loop shifts from a low to a relatively high pressure, which indicates the increase in mesopore size from 2.5 nm for Z-G-130 to 4.3 nm for Z-A-130. The shape of the hysteresis loop shows a change from H2 to H1, which indicates the change from ink-bottle-like mesopores to slit-like mesopores [26]. Higher crystallization temperature also benefits the formation of larger mesopores.

Based on our previous experimental results [19], we can speculate on the formation mechanism of the mesopores within the meso-microporous composites. MFI zeolite primary units and their aggregates in the zeolite precursor sol pack closely in the xerogel during the vacuum drying process. Pores within the xerogel should have a narrow size distribution since the particle size of the precursor sol is uniform. During the solvo/hydrothermal crystallization process, primary units and

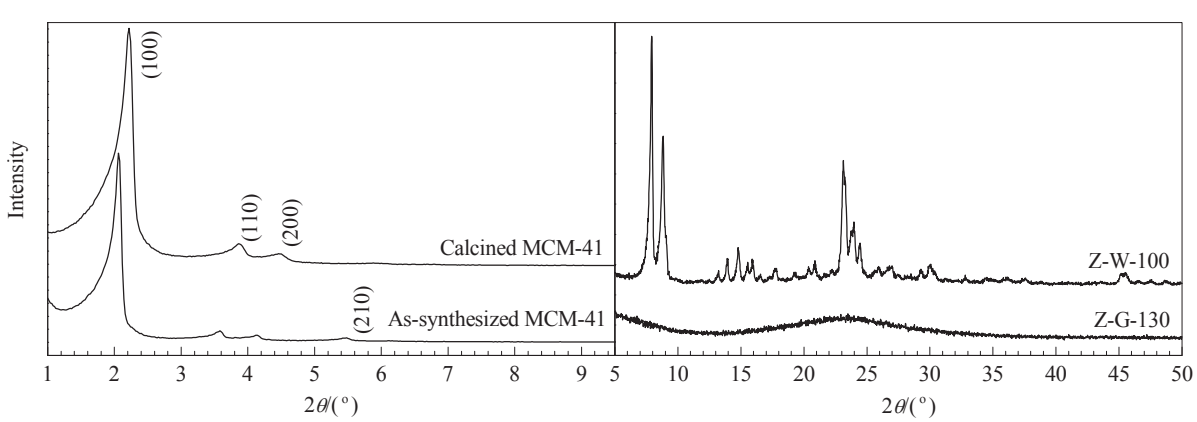

Fig. 1. XRD patterns of the studied samples.

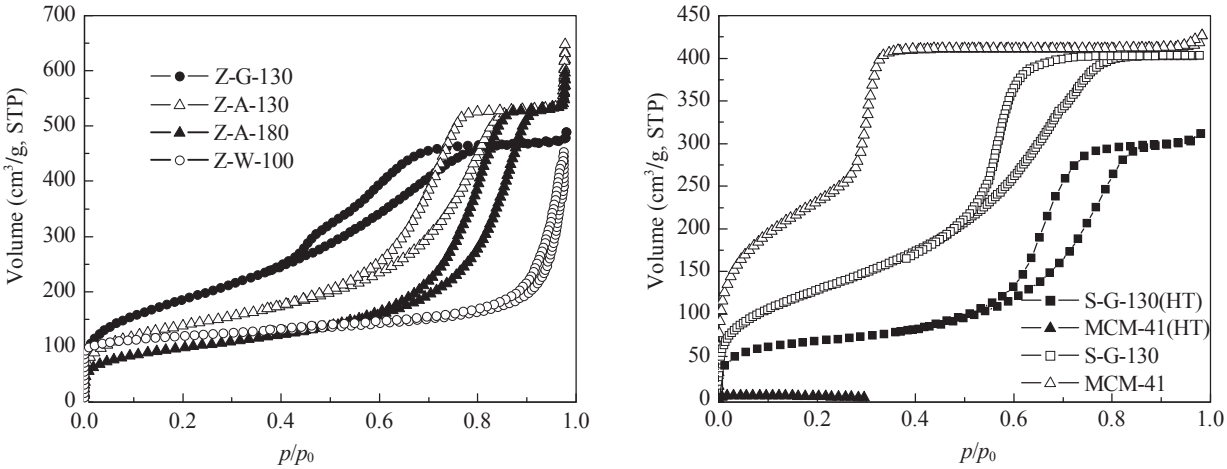

Fig. 3. N_2 adsorption/desorption isotherms of the studied samples. HT represents hydrothermal-treated samples at 180 °C.

their aggregates are the source of the alumina-silica species and the nuclei of the zeolite crystals, respectively. Therefore, the intermolecular action of the crystallization medium (mainly hydrogen band) affects directly the diffusion of species, sequentially zeolite growth process. Thus zeolite nanocrystals of different sizes form within the xerogel and intergrow into the walls of the final products because of the existence of a supersaturated alumina-silica species within the xerogel. The mesopores within the meso-microporous composites are interspaces between the zeolite nanocrystals. Compared to glycerol and glycol, water supplies a higher solubility and diffusion rate for the alumina-silica species. The uniformity of the mesopore size in Z-W-100 is destroyed by the rapid zeolite growth process. In our previous work [21], uniformly-sized mesopores (4.5 nm) were obtained by hydrothermal crystallization at 80 °C. SEM images showed that the size of the spherical nanoparticles increased obviously from 10 nm (80 °C) and 30 nm (100 °C) to 200 nm (130 °C).

The hydrothermally-treated S-G-130 sample (S-G-130(HT) sample) retains its mesopores with a narrow size distribution and most pore volume. Its mesopore size increases slightly from the original 3.1 nm to 3.8 nm accompanied by a decrease in BET specific surface area (Fig. 4 and Table 1). Compared to S-G-130(HT), hydrothermal-treated MCM-41 at 180 °C for 12 h disappears its mesoporous structures. Its BET specific surface area decreases obviously from the original 847.8 m^2/g to 12.2 m^2/g. These results show that the meso-microporous composite has remarkably improved hydrothermal stability compared to the conventional mesoporous material. From the large increase in micropore size of the S-G-130(HT) sample we believe that some micropores extend and fuse because of Si-O-Si hydrolysis during hydrothermal treatment. However,

Table 1 Specific surface areas and pore structural data of the studied samples

Sample	A_{BET} (m^2/g)	V_{meso} (cm^3/g)	V_{micro} (cm^3/g)	D_{meso} (nm)	D_{micro} (nm)
S-G-130	473.1	0.48	0.14	3.1	0.57
S-G-130(HT)	243.3	0.35	0.11	3.8	1.01
MCM-41	847.8	0.27	0.36	2.6	wide
Z-G-130	675.5	0.66	0.06	2.5	0.53
Z-A-130	499.3	0.77	0.04	4.3	0.56
Z-A-180	354.6	0.77	0.03	6.2	0.57
Z-W-100	464.9	0.48	0.11	wide	0.54

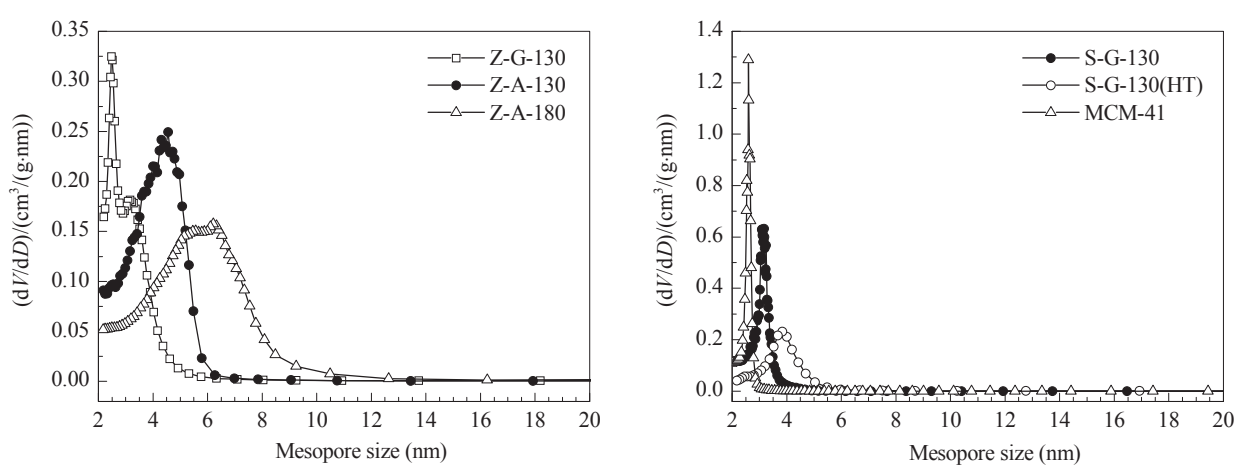

Fig. 4. Mesopore size distributions of the studied samples.

the destruction process is suppressed because of the existence of zeolite structures. Moreover, mesopore walls with zeolite structures were found to have higher mechanical strength because hydrothermal stability testing was carried out in an autoclave at 180 °C where 1 MPa exists.

2.4 Catalytic cracking performance of the studied samples

We investigated catalytic cracking activities and selectivities of different samples using 1,3,5-triisopropylbenzene as a reactant. No cracking products were detected over inert quartz sand under the reaction conditions, so a thermal cracking process can be ignored. From Fig. 5 the meso-microporous composites are shown to have similar catalytic activities upon an increase in the injection number whereas the catalytic activity of the commercial HZSM-5 zeolite (Si/Al = 25, Nankai University) decreases rapidly. Since the kinetic diameter of 1,3,5-triisopropylbenzene is ca. 0.74 nm, which is larger than the size of the micropores within the HZSM-5 zeolite, the acidity sites on the external surface of the HZSM-5 zeolite contributes to the catalytic cracking activity. Coke deposition on these acid sites results in a rapid deactivation of the HZSM-5 zeolite. The catalytic cracking activities of the meso-microporous composites results from the acid sites on the mesopore walls where coke deposition is hindered by the limited mesopore size.

Table 2 shows the catalytic cracking product distributions and conversions of 1,3,5-triisopropylbenzene over different samples after 20 injections. The conversion of 1,3,5-triisopropylbenzene and the selectivity for cumene over Z-G-130 sample with a mesopore size of 2.5 nm reaches 94.2% and 42.9%, respectively. For Z-A-130 sample with the mesopore size of 4.3 nm, these values are only 41.2% and 8.9%, respectively. On one hand, the smaller mesopore size of Z-G-130 sample is closer to the kinetic diameter of 1,3,5-triisopropylbenzene, which benefits the pre-activation of the reactant molecules. On the other hand, the cracking products diffuse more rapidly within larger mesopores resulting in a low selectivity for cracking products with small molecular weights.

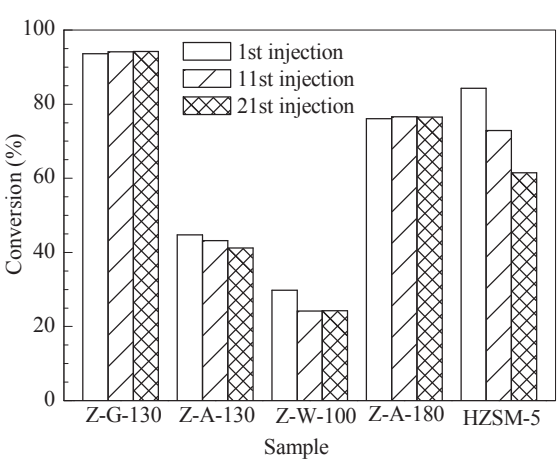

Fig. 5. Catalytic cracking conversion of 1,3,5-triisopropylbenzene over different samples after different number of injections. Reaction conditions: 400 °C, 50 mg catalyst, 0.1 μl reactant.

Table 2 Catalytic cracking product distributions and conversions of 1,3,5-triisopropylbenzene over different samples

Sample	Selectivity (%)			Conversion
	Benzene	Cumene	DIPB[b]	(%)
Z-G-130	1.8	42.9	55.3	94.2
Z-A-130	0.1	8.9	91.0	41.2
Z-A-180	0.3	18.5	81.2	76.5
Z-W-100	0.4	8.0	91.5	24.3
HZSM-5	65.5	3.7	30.8	61.5

[a]Results of the 21st injection; [b]Diisopropylbenzene.

The difference in the catalytic performance between Z-A-130 sample and Z-A-180 sample mainly results from the number of acid sites within the catalysts since the pre-activation of reactant molecules is not obvious within the larger mesopores. Z-A-180 sample that was prepared at a higher crystallization temperature has a higher zeolite crystalline ordering (i.e. more acid sites). Therefore, higher conversion is obtained over Z-A-180 sample. It should be noted that the commercial HZSM-5 zeolite has a higher catalytic activity. Considering the difference in Si/Al ratio between the meso-microporous composites (Si/Al=50) and the commercial HZSM-5 (Si/Al=25), the TOFs of 1,3,5-triisopropylbenzene over the meso-microporous composites are higher than that over the commercial HZSM-5. We can reasonably presume from the change in catalytic activity (Fig. 5) that a further deactivation will occur over commercial HZSM-5 because of coke deposition onto the surface acid sites.

3 Conclusions

A series of silica and aluminosilicate meso-microporous composites were prepared by solvo/hydrothermal crystallization of the xerogel that was converted from a uniformly-sized MFI zeolite precursor sol. Compared to mesoporous MCM-41, the silica meso-microporous composite shows remarkably improved hydrothermal stability because of the existence of zeolite structures. We also found that aluminosilicate meso-microporous composites show higher catalytic activity and ability against deactivation compared to commercial HZSM-5 zeolite in the catalytic cracking reaction of 1,3,5-triisopropylbenzene. Based on the characterization results of the meso-microporous composites prepared under different conditions such as crystallization solvent and temperature, work is being done to establish a new model of zeolite structure growth for directing synthesis of hierarchical porous catalysts applied in a certain reaction.

Acknowledgments

The authors gratefully acknowledge Dr. Min ZHANG for fruitful discussions, Senior Engineer Shishan SHENG and Associate Prof. Wenling CHU for the measurement of N_2 adsorption/desorption isotherms.

References

1 Corma A. *Chem Rev*, 1997, **97**: 2373
2 Kresge C T, Leonowicz M E, Roth W J, Vartuli J C, Beck J S. *Nature*, 1992, **359**: 710
3 Beck J S, Vartuli J C, Roth W J, Leonowicz M E, Kresge C T, Schmitt K D, Chu C T W, Olson D H, Sheppard E W, Mccullen S B, Higgins J B, Schlenker J L. *J Am Chem Soc*, 1992, **114**: 10834
4 Tao Y S, Kanoh H, Abrams L, Kaneko K. *Chem Rev*, 2006, **106**: 896
5 Liu Y, Zhang W Z, Pinnavaia T J. *Angew Chem*, *Int Ed*, 2001, **40**: 1255
6 Liu Y, Pinnavaia T J. *J Mater Chem*, 2002, **12**: 3179
7 Zhang Z T, Han Y, Xiao F S, Qiu S L, Zhu L, Wang R W, Yu Y, Zhang Z, Zou B S, Wang Y Q, Sun H P, Zhao D Y, Wei Y. *J Am Chem Soc*, 2001, **123**: 5014
8 Han Y, Xiao F Sh. *Chin J Catal*, 2003, **24**: 149
9 Jacobsen C J H, Madsen C, Houzvicka J, Schmidt I, Carlsson A. *J Am Chem Soc*, 2000, **122**: 7116
10 Schmidt I, Boisen A, Gustavsson E, Stahl K, Pehrson S, Dahl S, Carlsson A, Jacobsen C J H. *Chem Mater*, 2001, **13**: 4416
11 Tao Y S, Kanoh H, Kaneko K. *J Am Chem Soc*, 2003, **125**: 6044
12 Li W C, Lu A H, Palkovits R, Schmidt W, Spliethoff B, Schuth F. *J Am Chem Soc*, 2005, **127**: 12595
13 Xiao F S, Wang L F, Yin C Y, Lin K F, Di Y, Li J X, Xu R R, Su D S, Schlogl R, Yokoi T, Tatsumi T. *Angew Chem*, *Int Ed*, 2006, **45**: 3090
14 Wang H, Pinnavaia T J. *Angew Chem*, *Int Ed*, 2006, **45**: 7603
15 Choi M, Cho H S, Srivastava R, Venkatesan C, Choi D H, Ryoo R. *Nature Mater*, 2006, **5**: 718
16 Choi M, Na K, Kim J, Sakamoto Y, Terasaki O, Ryoo R. *Nature*, 2009, **461**: 246
17 Janssen A H, Koster A J, de Jong K P. *Angew Chem*, *Int Ed*, 2001, **40**: 1102
18 Groen J C, Moulijn J A, Perez-Ramirez J. *J Mater Chem*, 2006, **16**: 2121
19 Han W, Jia Y X, Yao N, Yang W S, He M Y, Xiong G X. *J Sol-Gel Sci Technol*, 2007, **43**: 205
20 Han W, Jia Y X, Xiong G X, Yang W S. *Stud Surf Sci Catal*, 2007, **165**: 515
21 Han W, Jia Y X, Xiong G X, Yang W S. *Sci Technol Adv Mater*, 2007, **8**: 101
22 de Moor P P E A, Beelen T P M, Komanschek B U, Diat O, van Santen R A. *J Phys Chem B*, 1997, **101**: 11077
23 de Moor P P E A, Beelen T P M, van Santen R A. *J Phys Chem B*, 1999, **103**: 1639
24 On D T, Kaliaguine S. *J Am Chem Soc*, 2003, **125**: 618
25 Jansen J C, van der Gaag F J, van Bekkum H. *Zeolites*, 1984, **4**: 369
26 Sing K S W, Everett D H, Haul R A W, Moscou L, Pierotti R A, Rouquerol J, Siemieniewska T. *Pure Appl Chem*, 1985, **57**: 603